Journal of Materials Science: Materials in Medicine (2018)29:158
https://doi.org/10.1007/s10856-018-6166-x

DELIVERY SYSTEMS

Original Research

In situ-forming and pH-responsive hydrogel based on chitosan for vaginal delivery of therapeutic agents

Esmat Jalalvandi[1] · Amin Shavandi[2]

Received: 20 August 2018 / Accepted: 10 October 2018

Abstract

One of the important routes of drug administration for localized delivery of contraceptives and cervical cancer treatment agents is vaginal canal. Due to the low pH of vagina, a pH-responsive drug delivery system was developed. This hydrogel was synthesized based on a mucoadhesive biopolymer, chitosan (CS), that promotes the interaction between the hydrogel and mucosal surface of the vagina, potentially increasing the residence time of the system. This injectable hydrogel was formed via acid-labile Schiff-base linkages between free amine groups and aldehyde functionalities on modified chitosan. A novel approach was taken to add aldehyde functionalities to chitosan using a two-step reaction. Two types of slow and fast degrading hydrogels were prepared and loaded with iron (II) gluconate dihydrate, a non-hormonal spermicide, and doxorubicin hydrochloride, an anti-cancer drug. The release profiles of these drugs at different pH environments were assessed to determine the pH-dependent release mechanism. Mechanical properties, swell-ability and degradation rate of these matrices were studied. The cross-linking density of the hydrogel as well as pH changes played an important role in the characteristic of these hydrogels. The hydrogels degraded faster in lower pH, while the hydrogel with lower cross-linking density showed longer gelation time and faster degradation rate compared to the gel with higher cross-linking density. *In vitro* cytotoxicity assessment of these hydrogels in 48 h indicated the non-toxic effect of these hydrogels toward mesenchymal stem cells (MSCs) in the test period.

✉ Esmat Jalalvandi
e.jalalvandi@hw.ac.uk

[1] Department of Mechanical Engineering, College of Engineering and Mathematical Sciences, University of Vermont, Burlington, VT 05405, USA

[2] Department of Food Science, Centre for Bioengineering and Nanomedicine, University of Otago, Dunedin 9054, New Zealand

Published online: 22 October 2018

Graphical Abstract

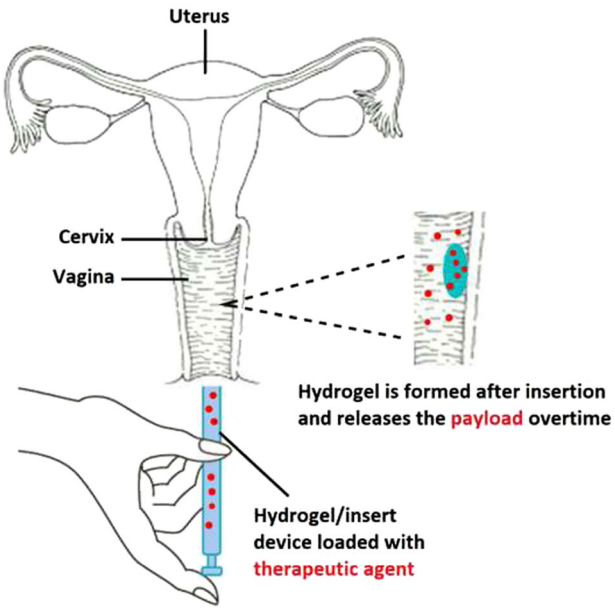

1 Introduction

Progress in drug delivery has led to a wider choice of sites for drug administration. Intravaginal administration is an important route of drug delivery for local or systemic diseases and contraceptives [1]. This mucosal route of drug delivery allows women to self-administer contraceptives or other medications [2, 3]. The vaginal epithelium is highly permeable to small molecules and has a large surface area with high vascularization, which has the ability to bypass the hepatic first-pass effect [1, 4]. Localized vaginal delivery allows direct therapeutic action and reduces adverse effects and frequency of the dosage taken while limiting systemic drug toxicities by promoting the release of the drug directly to the target site [5, 6]. Due to ease of access and non-invasive implantation, vagina appears to be an ideal route for drug administration, in particular for cervical cancer treatment and contraception [2, 7]. Many different vaginal formulations including gels, creams, pessaries, suppositories, rings, films, and tablets have been developed to deliver drugs for different applications such as contraception and cancer treatment [8–10]. However, patient compliance, adverse effects, practicality, and biocompatibility are still the main concerns in the design of vaginal drug delivery systems [11, 12].

Cervical cancer is one of the most common cancers affecting women worldwide and it is particularly widespread in developing countries due to the lack of prevention programs [13, 14]. Many chemotherapeutic drugs including paclitaxel, topotecan, 5-fluorouracil, docetaxel, mitomycin, and doxorubicin hydrochloride (DOX) have been used to treat cervical cancer [15–20]. Vagina provides an easy way for the localized delivery of these chemotherapeutic drugs to the cervix directly. Moreover, many contraception methods such as condoms, intrauterine devices, spermicides, oral pills, and injectable hormonal contraceptives are available to women today. However, these methods are not easily accepted by all users due to their inconvenience and side effects such as increased rate of depression, weight gain, nausea, and headache [21, 22]. In addition, hormonal contraception may alter hormone levels, and possibly increase the risk of cervical and breast cancer among women who use this method for +5 years [23–25]. Therefore, non-hormonal contraceptives such as iron (II) glyconate dehydrate (FeGl) have been employed as alternative contraception method with less side effects [25, 26]. There is a need for design of a safe intravaginal delivery system with high acceptability among women to deliver non-hormonal contraceptives and/or cancer treatment drugs directly to the target site. The use of hydrogels for release of therapeutic agents have been investigated extensively. Depending on the intended site of use, these networks can be designed to be thermos-sensitive, pH-responsive, degradable, or mucoadhesive [27–30].

In the present study, a novel chitosan (CS)-based hydrogel/insert was designed to deliver a non-hormonal contraceptive, FeGl, and a cervical cancer treatment drug, DOX, to the vaginal canal. It was hypothesized that CS

interacts with mucosal surfaces (e.g., vaginal cavity) through an interaction with charged sugar groups such as sialic acid [31, 32], and therefore, hydrogels based on this mucoadhesive polymer could reside in mucosal environment of vagina, which might result in a prolonged drug release from these hydrogels [33, 34]. The hydrogels were prepared based on Schiff-base chemistry berween a novel aldehyde-modified CS and *N*-succinyl CS. Schiff-base linkages can be cleaved via hydrolysis of the imine bond especially at low pH. This ability to degrade at low pH is useful in the degradation process of these gels inside vagina since vaginal cavity has lower pH (4–4.5) compared to the rest of the body (7.4) [35, 36]. Gelation kinetic, rheological behavior, cytotoxicity, degradation, and swell ability of these hydrogels were studied. The release profiles of FeGl and DOX were also assessed in different pH environments. The results showed that these hydrogels are pH-sensitive and exhibited no toxicity toward MSC line. Degradation and gelation time of these hydrogels depend on the cross-linking density, which could be controlled by the density of functional groups during the synthesis of precursors.

2 Materials and methods

2.1 Materials

Chitosan (CS, medium molecular weight, M_w: 190–310 kDa), dimethylformamide (DMF), dimethyl sulfoxide (DMSO), glycidol, acetic acid (6 N), sodium periodate, DOX, iron (II) glyconate dehydrate (FeGl), thiazolyl blue tetrazolium bromide (MTT), penicillin–streptomycin, and trypsin-EDTA were obtained from Sigma-Aldrich, USA. Succinic anhydride (99%) and sodium hydroxide were acquired from Acros Organic, USA. Mesenchymal stem cells (MSCs, passage 5), fetal calf serum (FCS), and minimum essential media (MEM) was purchased from Gibco and dialysis tubing was acquired from Spectra/Por (MWCO 6000–8000 RC). All chemicals were used without further purification.

2.2 Synthesis of precursors

A novel aldehyde-functionalized CS (Al-CS) was produced in two steps. First, CS (10.0 g, 58.6 mmol) was dissolved in a mixture of distilled water and acetic acid (200:3.0 ml). Glycidol (11.0 ml, 164 mmol) was then added dropwise to the solution at 60 °C and stirred for 20 h. The final mixture was centrifuged at 2000 r.p.m. for 5 min at 30 °C to remove the undissolved particles. The clear solution was precipitated in cold ethanol to remove unreacted glycidol monomers. The filtrate was collected, re-dissolved in distilled water, and dialyzed against water for 24 h. After lyopholization at −40 °C, glycidol-modified CS (G-CS) was collected in 79% yield. In the next step, G-CS (5.0 g, 24.6 mmol) was dissolved in distilled water (100 ml) and sodium periodate (5.0 g, 23.4 mmol) was dissolved in water and added dropwise to G-CS solution. The mixture was stirred at room temperature (22 °C) for 5 h and then dialyzed against water for 48 h. After the lyophilization, aldehyde-functionalized CS, Al-CS, was collected in 53% yield.

CS was also modified with succinic anhydride to produce a water-soluble derivative of CS, namely *N*-succinyl-CS according to the previous reports [37, 38]. Briefly, CS (10.0 g, 58.6 mmol) was dispersed in DMF (200 ml) and succinic anhydride (14 g, 140 mmol) was added to the mixture and heated up to 125 °C for 5 h. The mixture was filtered and washed with ethanol. The dried product was re-dissolved in NaOH solution (5 w/v %, 500 ml) and stirred at 65 °C for 20 h under N_2 protection. The final solution was filtered and placed in dialysis tubing for further purification. Lyophilization of the dialyzed solution resulted in *N*-succinyl-CS production with 66% yield.

2.3 Hydrogel preparation

Individual solutions of Al-CS and *N*-succinyl-CS (3 or 5 w/v %) were prepared in PBS (pH 7.4) buffer and mixed in equal volumes (each 1 ml) at room temperature in 10 ml syringe tubes with the tips cut off and left for 10 h to set. Gel 3% was made by mixing Al-CS and *N*-succinyl-CS with 3 w/v % concentration, whereas gel 5% was made by mixing an equal volume of the Al-CS and *N*-succinyl-CS with 5 w/v % concentration. The final shape of each hydrogel was cylindrical with the following dimensions: height: 2 cm, diameter: 1.2 cm. The Schiff-base reaction between free amine groups of *N*-succinyl-CS and aldehyde functionalities of Al-CS formed the cross-linked networks. Formation of Schiff base or imine is a reversible reaction, which is ideal for the degradation of hydrogel networks especially at lower pH due to the sensitivity of imine bond to the low pH [39, 40].

2.4 Characterization

Fourier transform infrared (FTIR) spectra were recorded on a Bruker optic Alpha-p spectrometer with a diamond attenuated total reflectance top plate. Nuclear magnetic resonance (NMR) spectra were recorded on a Bruker AVANCEIII spectrometer at 500 MHz using D_2O solvent at 30 °C. The viscosity of the polymer solutions and gelation kinetic of the resultant hydrogels were analyzed using a Thermo Haake Rheostress (RS1, Thermo Electron Corporation, MA) at 37 °C. The rheometer was equipped with a cone geometry (Ø = 20 mm, 1° cone angle) and a Peltier plate. Apparent viscosity

was measured over shear rate ranging from 1 to 100 (s^{-1}), using non-cross-linked precursor solutions. Gelation kinetics for each hydrogel was studied by performing oscillatory time sweeps at 10% radial strain and constant frequency of 1 Hz. Equal volumes of the precursors were loaded onto the plate of the rheometer and storage modulus (G′) as well as loss modulus (G″) were recorded.

2.5 Degradation and swelling

In vitro degradation and swelling measurements were performed for both hydrogel sets in an aqueous medium at different pHs (7.4 and 4.5) at 37 °C according to the previously reported procedures [27, 41]. The lower pH medium represented the pH of vaginal cavity [35, 36]. Hydrogels were prepared according to the method in 'Hydrogel preparation' section. Each hydrogel sample was immersed in buffer solution (50 ml, pH 7.4 or 4.5) at 37 °C, and the medium was periodically renewed with the fresh buffer. The degradation study was carried out in triplicates ($n = 3$) using a stainless steel basket shown in Fig. 4 and each group was being utilized every day. The hydrogel samples were removed from the buffer solution, lyophilized, and the weight loss calculated. Swelling tests were carried out in triplicates ($n = 3$). The dry gel samples were weighed and immersed in a vial filled with PBS solution (pHs 7.4 and 4.5) and incubated at 37 °C. The change in weight of the gels was recorded at regular intervals by removing the gels from the vial, blotting excess PBS, and then re-weighing [39].

2.6 In vitro cytotoxicity

MSC cells were grown in sterile 75 cm^2 tissue culture flasks in MEM, supplemented with 10 v/v % FCS, 1% penicillin–streptomycin (10,000 mg/l). The cells were maintained at 37 °C in a humidified atmosphere in the presence of 5% CO_2/air to reach a confluent layer. The cultured monolayer was trypsinized and used for in vitro biocompatibility test. The viability of MSC cells was evaluated in the presence of gel 3% and gel 5% using MTT assay [42]. Components of each hydrogel set was prepared in MEM with related concentration (0.5 ml). The solutions were placed inside culture inserts (8 µm pore size, BD Falcon, USA) and mixed to form the corresponding hydrogel [27, 39]. Once cross-linked, the inserts were transferred to pre-seeded wells (0.5×10^5 cells/ml, 24-well polystyrene plates) and the plate was incubated at 37 °C and 5% CO_2. The cell viability was determined after 48 h incubation for each hydrogel set compared to the normal growth control. After 48 h, the culture inserts and the media were removed, and MTT solution (5 mg/ml, 250 µl) was added to each well and incubated for 3 more hours. MTT was metabolically reduced by viable cells to a blue-violet formazan, which was then dissolved in DMSO (250 µl). The absorbance of each well was measured at 570 nm to determine the number of viable cells using ultraviolet (UV) plate reader (H1Synergy, BioTek). The following equation was employed to calculate cell viability for each hydrogel [42], where A is the absorbance of the corresponding wells at 570 nm.

$$\text{Cell viability } \% = \frac{A_{\text{test component}} - A_{\text{blank or media only}}}{A_{\text{normal growth cells}} - A_{\text{blank or media only}}} \times 100.$$

2.7 Drug loading and release study

Individual solutions of Al-CS and *N*-succinyl-CS were prepared in PBS (pH 7.4) with two different concentrations (3 and 5 w/v %). FeGl (50 mg) was dissolved in the solution of Al-CS (1 ml) and the final solution was transferred to the syringe mold and mixed with the *N*-succinyl-CS solution (1 ml) to form the cross-linked matrix. DOX was encapsulated in the gel matrix in the similar fashion. Al-CS (1 ml) was mixed with DOX (2 mg) and transferred to the mold to mix with *N*-succinyl-CS and form the hydrogels loaded with DOX. Hydrogels loaded with FeGl or DOX ($n = 3$) were left for 10 h to set followed by immersing each gel in separate medium (20 ml, pHs 7.4 and 4.5) at 37 °C. At specific time intervals, the PBS was replaced with the same amount of fresh buffer and was analyzed by a UV spectrophotometer (H1Synergy, BioTek). The media removed from FeGl-loaded gels were analyzed at 380 nm, whereas DOX-loaded networks were examined at 485 nm to determine the absorption and consequently the amount of FeGl or DOX released from the hydrogels. The cumulative release of these two drugs were calculated using their calibration curves obtained from the various concentrations of these drug solutions. Blank hydrogels, with no drug loaded, were used as control samples in this study.

2.8 SEM images

Scanning electron microscope (SEM) images from freeze-dried gels were obtained using JJEOL 2200FS scanning transmission electron microscope JEOL Ltd, Tokyo, Japan) operating at 15 kV and a Direct Electron DE-20 detector (Direct Electron LP, California, USA) The lyophilized hydrogel samples were mounted onto one large aluminum specimen stub in puddles of liquid graphite, sputter-coated with gold and palladium and imaged.

2.9 Statistical analysis

Data are expressed as the mean ± standard deviation ($n = 3$). The results were statistically analyzed by one-way analysis of variance with Bonferroni post-test and the statistical significance was set at $P \leq 0.05$.

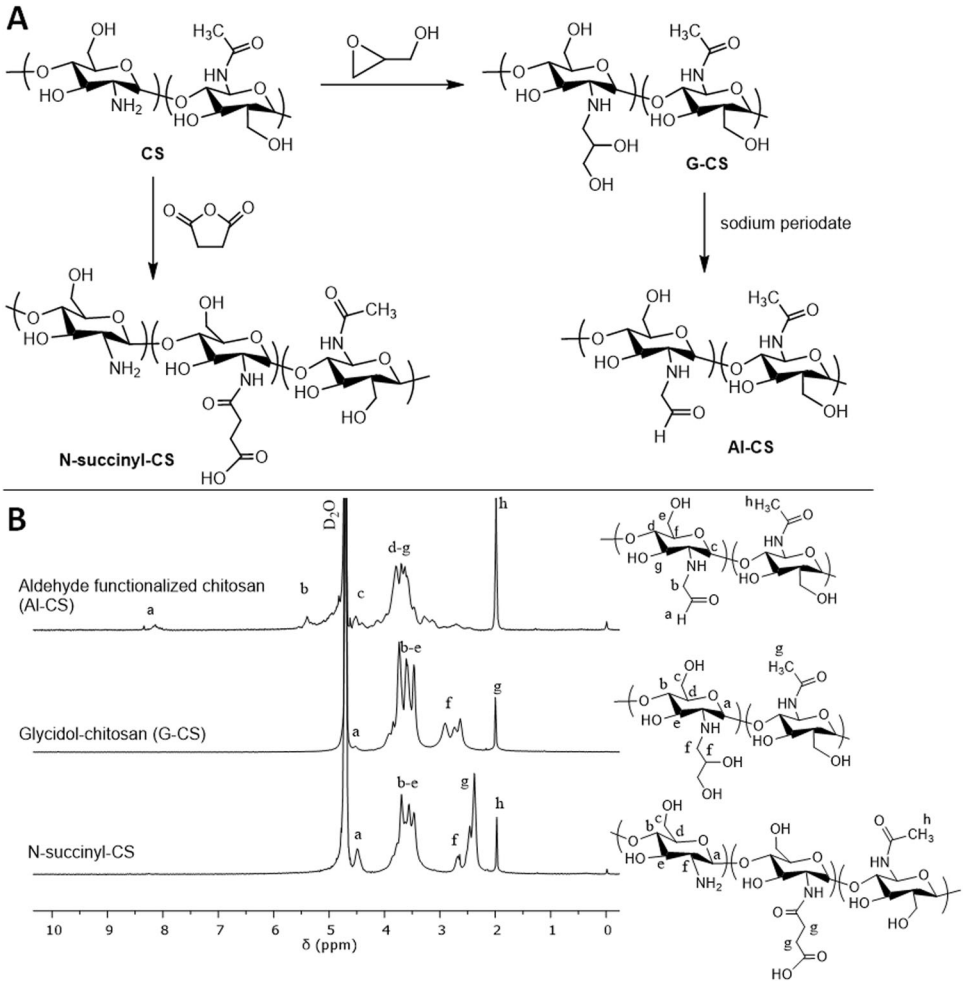

Fig. 1 **a** Schematic synthetic route of *N*-succinyl-CS and Al-CS using succinic anhydride, glycidol, and sodium periodate, respectively. **b** Proton NMR spectra of the *N*-succinyl-CS, glycidol-modified chitosan (G-CS), and aldehyde-modified chitosan (Al-CS) in D_2O solvent at 30 °C

3 Results

3.1 Synthesis of precursors

Figure 1 shows the schematic synthetic routes of *N*-succinyl-CS, G-CS, and Al-CS, and their ^{1}H NMR spectra. In the ^{1}H NMR spectrum of *N*-succinyl-CS, the signal centered at 1.9 p.p.m. corresponds to the proton of the acetyl group of acetylated units of CS (labeled as h), while the peak at 2.8 p.p.m. corresponds to the proton of the glucosamine ring representing the number of free amine groups. The signals between 3.3 and 3.9 p.p.m. can be attributed to the four protons of CS backbone (labeled as b–e). The ^{1}H NMR spectrum of G-CS revealed complete modification of the free amine groups through reacting with the epoxide. The appearance of a broad signal between 2.5 and 3 p.p.m. (labeled as f) corresponding to the protons of pendant group in G-CS confirmed the formation of G-CS. The ^{1}H NMR spectrum of Al-CS shows new signals at 5.3 and 8.2 p.p.m. that represent protons of aldehyde moieties in this polymer. FTIR spectra of two precursors, *N*-succinyl-CS, and Al-CS, are presented in Fig. 2. In FTIR spectrum of *N*-succinyl-CS, the band at 1410 cm^{-1} is due to asymmetric stretching of $-COO^-$ ions of *N*-succinyl-CS. This absorption band provides a direct indication of *N*-succinyl-CS formation. In addition, a new peak of secondary amine emerged at 1550 cm^{-1} further confirmed the formation of *N*-succinyl-CS [43]. In the FTIR spectrum of Al-CS, the stretching band at 1720 cm^{-1}, was related to C = O, conjugated aldehyde [27].

3.2 Rheological measurements

Viscosity values for Al-CS and *N*-succinyl-CS polymers with two different concentrations (3 and 5 w/v %) are presented in Fig. 3a. In general, viscosities of Al-CS solutions (3 and 5 w/v %) were slightly lower compared to the *N*-succinyl-CS solutions. This could be due to a two-step reaction process to synthesize Al-CS including an oxidation step. Chemical modification of the polymers might result in degradation and reduction of final molecular weight of the polymer, which consequently impacts the viscosity of materials. The viscosity of 5 w/v % *N*-succinyl-CS is higher than the 3 w/v % solution as expected [42]. Gelation kinetics for gel 3% and gel 5 % were studied by oscillating a

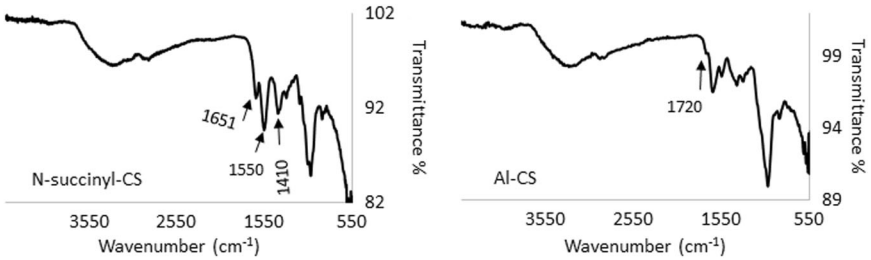

Fig. 2 FTIR spectra of *N*-succinyl-CS (left) and Al-CS (right)

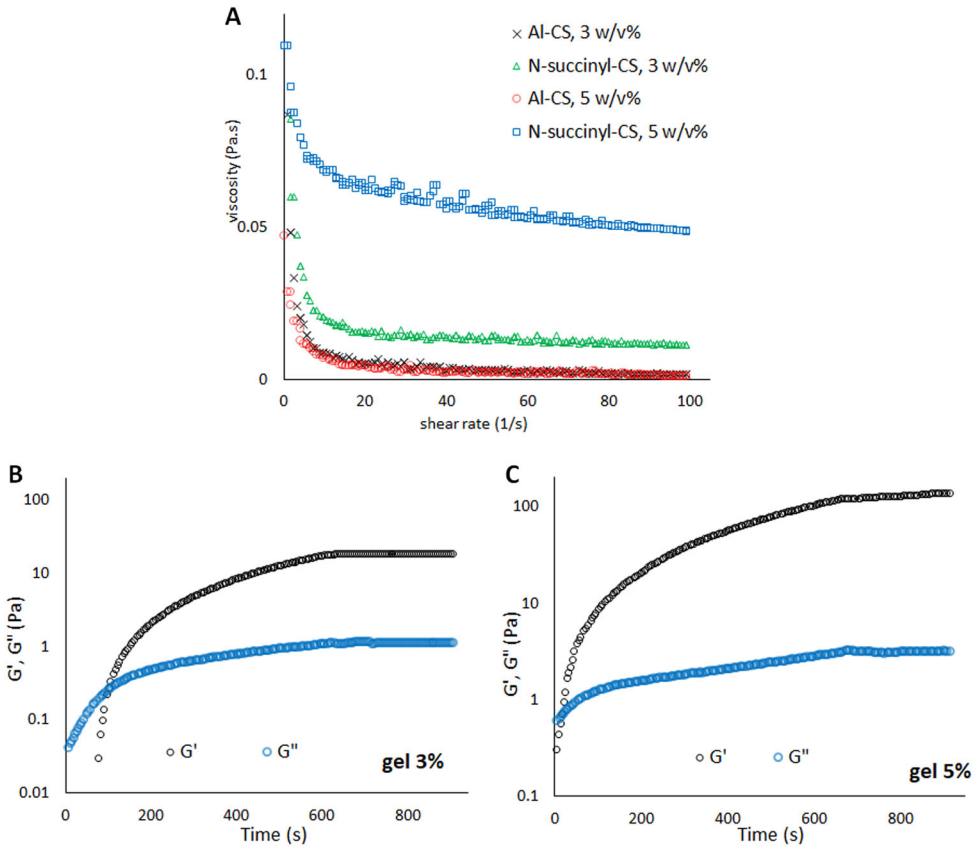

Fig. 3 **a** Viscosity values vs shear rate for the components of both hydrogels at 37 °C. **b** Time sweep performed on components of gel 3% and **c** gel 5% (right), at 37 °C and 1 Hz frequency. The cross-over point of G′ and G″ is defined as the gelation time

shear force during the cross-linking process (Fig. 3b, c). Storage modulus, G′, and loss modulus, G″, were measured for 15 min at 37 °C. At the very beginning, in both gel 3% and gel 5%, G′ was lower than G″ and the systems behaved like viscous fluids. Formation of the cross-linked network over time, resulted in a speedy rise of G′ and G″. The cross-over point between G′ and G″ (G′ > G″) is known as the gelation time and was observed for the gel 5% at 43 s, while it was at 77 s for the gel 3%.

3.3 In vitro hydrolytic degradation and swelling tests

Hydrogels with potential biomedical applications would be exposed to biological fluids, therefore, it is important to study their swelling behavior. Swelling ratio depends on the nature of the polymer and their ability to expand, degree of cross-linking as well as external factors such as temperature and pH [27]. Figure 4 illustrates the results of swelling studies in different pHs (7.4 and 4.5) for gel 3% and gel 5%. Overall, the swelling index increases with time, first rapidly and then gradually, reaching the maximum constant swelling in almost 2 h for both gels. It was observed that gel 3% with lower cross-linking density showed higher amount of water adsorbed, while both gels in lower pH medium had slightly higher swelling ratio compared to the gels in neutral medium (pH 7.4). This could be due to ionization of unreacted amine groups on *N*-succinyl-CS in lower pH, which affect the swelling index of the gels in acidic condition [44]. Figure 4 also shows the degradation profiles of these networks. Gel 3% with lower degree of cross-linking degraded faster than gel 5% as expected. Both gels show

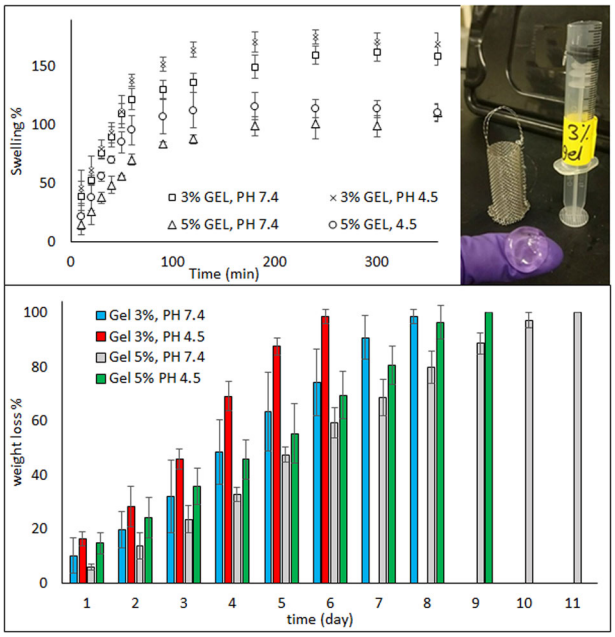

Fig. 4 Swelling test and weight loss study for gel 3% and gel 5% in pHs 4.5 and 7.4 at 37 °C ($n = 3$). A 10 ml syringe tubes with the tips cut off was used as a mold for hydrogel fabrication and a stainless steel assembled into a basket shape was used to immerse the gels in medium to measure the degradation rate

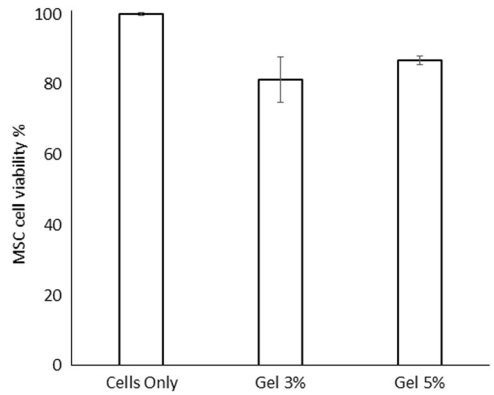

Fig. 5 Cell viability results using MTT assay when the statistical significance was set at $P \leq 0.05$. MSC cells showed >80% viability when exposed to gel 3% ($P = 0.204$) and gel 5% ($P = 0.258$)

faster degradation rate in pH 4.5 (representing pH of vagina) compared to pH 7.4 medium. This is due to the sensitivity of Schiff-base linkages to acidic conditions. Schiff-base linkages are cleaved via hydrolysis of the imine bond especially at low pH [27, 39, 40].

3.4 In vitro cytotoxicity test

Figure 5 shows the viability of MSC cells after being exposed to the hydrogels for 48 h. Both hydrogels, gel 3% and gel 5%, exhibited >80% cell viability and are considered non-cytotoxic (International Organization for Standardization, Part 5: Tests for in vitro cytotoxicity of medical devices, ISO 10993-5:2009 guidelines) [42].

3.5 In vitro release of FeGl and DOX

Hydrogels loaded with either DOX or FeGl were prepared according to the method described in section 2.7. The cumulative release of DOX and FeGl was calculated individually and plotted vs time intervals for gel 3% and gel 5% at 37 °C in two different media (pHs 7.4 and 4.5). The calibration curves were plotted by measuring the absorbance of different concentrations of FeGl and DOX, individually at 380 and 485 nm, respectively (Fig. 6). These calibration curves were used to calculate the amount of FeGl and DOX released from the gels in the specific time intervals.

Figure 7 shows the release profiles of FeGl from gel 3% and gel 5% in two different media (pHs 7.4 and 4.5) at 37 °C (chemical structure of FeGl is shown in Fig. 8b). For FeGl, the release was completed from gel 5% at pH 7.4, almost in 42 h. This time was shorter for gel 3% at pH 4.5 with only 10 h. Figure 7 also represents the release profile of DOX from gel 3% and gel 5% in two different media (pHs 7.4 and 4.5) at 37 °C. Compared to FeGl, a much steadier release profile was seen for DOX from gel 3% and gel 5%. DOX was released completely from gel 3% at lower pH in about 72 h, whereas the release time from gel 5% at neutral pH was reported in almost 132 h.

In Fig. 8, the formation of hydrogel via Schiff-base between aldehyde functionalities and free amine groups is shown. The imine bonds also form between aldehyde functionalities of Al-CS and amine groups of DOX molecules resulting in DOX-polymer conjugation. This is a reversible reaction and the link is hydrolyzed to release DOX molecules without changing its chemical structure. In contrast, no chemical interaction between FeGl molecules and polymer chains was expected.

3.6 SEM morphology

The hydrogels without loaded drugs were prepared, freeze-dried, and their cross-section morphology are shown in Fig. 9. The freeze-dried hydrogels clearly exhibited the presence of porous structures, which somewhat are artifacts of the drying process. Nevertheles, the porosity in these structures might provide room to accommodate the drug molecules inside these matrices.

4 Discussion

CS has low solubility in neutral pH (7.4) and in order to obtain a water-soluble precursor and prepare hydrogels, CS

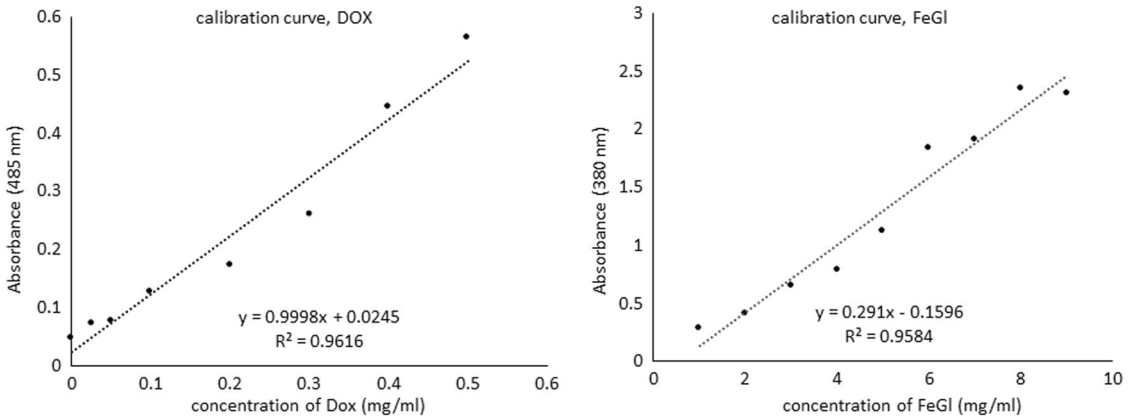

Fig. 6 Calibration curves for DOX and FeGl. Absorbance for different concentrations of DOX and FeGl was measured at 485 and 380 nm, respectively, to acquire a linear correlation. The trend-line equations were used to calculate the amount of drug released from each gel in release studies

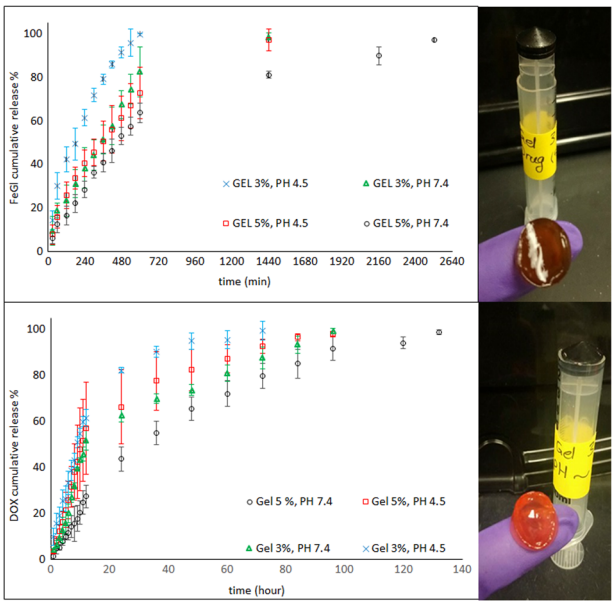

Fig. 7 The release profile of FeGl (up) and DOX (down) from gel 5% and gel 3% in different media (pHs 7.4 and 4.5) at 37 °C. Photos on the right show gel 3% loaded with FeGl (up) at time = 0 and DOX (down) at time = 0 of the release profiles ($n = 3$). Syringes with the tips cut-off were used as molds for hydrogel fabrication

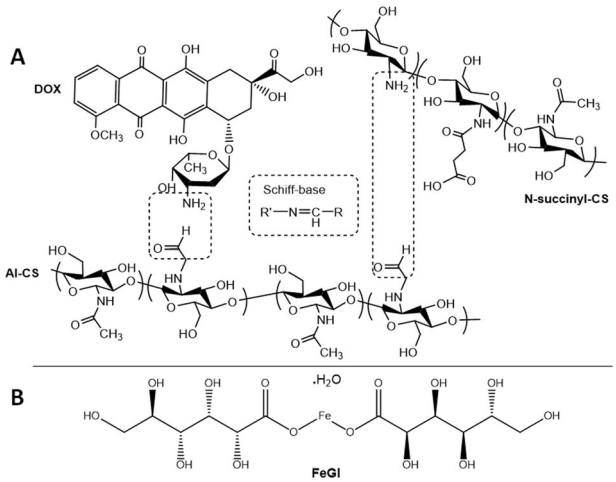

Fig. 8 **a** Formation of DOX-loaded hydrogel. Some of the aldehyde functionalities on Al-CS react with the free amine groups of DOX molecules via Schiff-base to obtain DOX-polymer conjugation and some of the aldehydes react with free amine groups of *N*-succinyl-CS to form the cross-linked network. The resultant hydrogel contains some free DOX molecules encapsulated in the matrix as well as some DOX conjugated to the polymer backbone. **b** The chemical structure of FeGl, non-hormonal contraceptive

was modified by succinic anhydride to produce *N*-succinyl-CS [45]. *N*-succinyl-CS is an acyl derivative of CS that is a biocompatible, biodegradable, and highly pH-sensitive [46]. The negatively charged carboxylate ions in *N*-succinyl-CS promote the mucoadhesive properties of this polymer [47]. This is an important asset in the design of current intravaginal drug delivery system, Since the vaginal cavity is a mucosal route of delivery [48], a hydrogel based on mucoadhesive polymers such as *N*-succinyl-CS could adhere to this route and potentially increase the residence time of the system in the vagina. *N*-succinyl-CS also possesses free amine groups available to bond with aldehyde functionalities through a Schiff-base reaction to form a cross-linked network (Fig. 8). To synthesize an aldehyde-functionalized CS, a novel two-step reaction was carried out. The first step was to solubilize CS using glycidol in which the amine groups of CS reacted with the epoxide to produce G-CS containing two neighboring hydroxyl groups. These neighboring OH groups were then oxidized using sodium periodate to introduce aldehyde functionalities on CS backbone and produce an aldehyde-functionalized precursor, Al-CS. FTIR and ^{1}H NMR spectra confirmed the production of the precursors, *N*-succinyl-CS, and Al-CS.

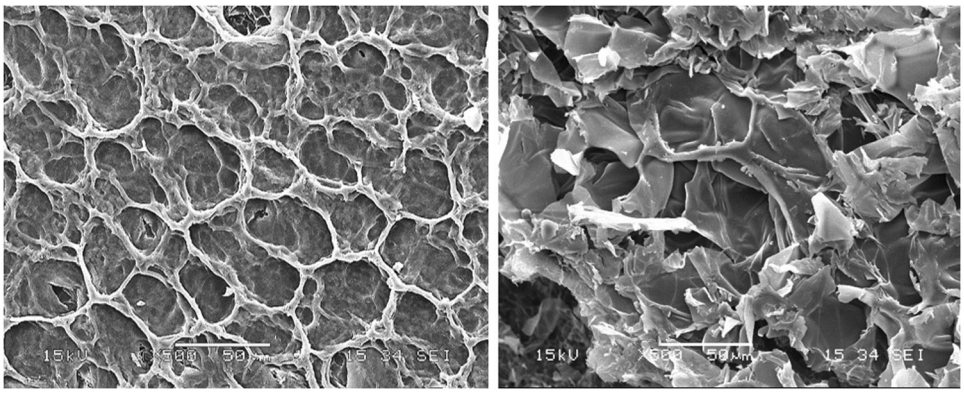

Fig. 9 SEM images of gel 3% (left), gel 5% (right) operating at 15 kV

Hydrogel formation through Schiff-base linkages was monitored using rheological analyses, where the values of G′ and G″ were recorded over 15 min. Longer gelation time for the gel 3% (77 s) was due to a lower concentration of the precursor solutions, which resulted in lower cross-linking density and longer reaction time compared to gel 5% (43 s) with higher density of aldehyde functionalities and free amines in the solution. Formation of these hydrogels in seconds demonstrates their ability as injectable hydrogels, also known as in situ-forming networks. Altering the concentrations of the precursors will affect the cross-linking density and subsequently impact the gelation time of these injectable systems. The results from degradation and swelling studies showed that these hydrogels are pH-responsive systems, which could degrade faster in environments with low pH (4.5) such as vagina. This is due to the presence of pH-sensitive imine linkage that hydrolyze rapidly at low pH [27, 39, 40].

Figure 7 shows the results of release studies for two different therapeutic reagents. Gel 3% has a lower cross-linking density than gel 5% and could offer a faster release of FeGl molecules through the matrix. Another reason for faster release of FeGl from gel 3% at lower pH is the nature of imide linkages that would hydrolyze faster in lower pH (4.5) than neutral medium (pH 7.4). The effect of hydrolysis was confirmed by degradation rate of each gel when gel 3% at lower pH and gel 5% at neutral pH were degraded in 6 and 11 days, respectively. Gel 5% in lower pH and gel 3% at neutral pH showed almost similar release profiles for FeGl where cumulative release was 100% after 24 h. In all cases, the burst effect can be observed for the first 12 h of the release of FeGl. This initial fast release may be due to the penetration of water molecules into the networks, as explained by swelling behavior, and consequently increasing the volume of matrices creating paths for FeGl molecules to escape. Longer release time of DOX compared to FeGl can be explained by the conjugation of DOX molecules to Al-CS (Fig. 8). The DOX-polymer conjugation could be responsible for the delay in the release time. Although, DOX was released in longer time compared to FeGl, all the gels showed the same pattern for release. Overall, gel 3% at low pH (4.5) showed the fastest release time for both DOX and FeGl while gel 5% at neutral pH demonstrated longer time to release DOX and FeGl. This was expected as imine linkages are more sensitive to lower pH and hydrolyze faster in this environment. Also, the cross-linking density plays an important role in the release profile where the hydrogel with higher cross-linking density (gel 5%) showed longer release time compared to gel 3% with lower cross-linking density. These results were in agreement with degradation rate of the hydrogels at different pHs where gel 5% at neutral pH showed the longest degradation time [39, 49].

Fast release of therapeutic reagent from hydrogels might be undesirable for many treatments, however, a fast release profile for FeGl, a non-hormonal contraceptive, could be beneficial as it acts immediately and locally. The FeGl-loaded hydrogel can be positioned prior to intercourse in the vagina to release the spermicide agent. This non-hormonal contraceptive agent is proved to cause structural damage to sperm and reduce its metabolic activity [25, 26, 50–52]. It targets the sperm tail and induces lipid peroxidation. Free oxygen radicals produced during this process result in cell damage [51, 53]. High level of fatty acids present in human sperms make these cells susceptible to the free radical species upon exposure to FeGl. This leads to a constant formation and decomposition of lipid peroxides and eventually causes structural damage, a decline in metabolic activity, and spermiostatic effects on sperm [26, 53]. On the other hand, longer release period of DOX from hydrogels compared to FeGl might be useful as DOX is a cancer treatment drug that eliminates cancerous cells locally in a long period of time. These hydrogels showed no significant toxicity toward MSC cell line after 48 h exposure to the cells, which proves the safety of these CS-based hydrogels for further in vivo studies.

5 Conclusion

Two sets of injectable hydrogels with different cross-linking densities were prepared via Schiff-base linkages. These imine bonds are pH-sensitive and hydrolyze faster in lower pH. Taking advantage of the low pH of vaginal canal, these hydrogels were designed to function as inserts for intravaginal delivery of therapeutics. The matrices were loaded with a common cervical cancer drug, DOX and a non-hormonal contraceptive, FeGl. The users could position these hydrogels in the vagina either prior to intercourse to release the spermicide agent or to release DOX at tumor site, directly. There is no need for removal of these devices after their functions as they are degradable, which could increase their acceptance among the users. Although a more in-depth cytotoxicity study employing more appropriate cell line as well as mucoadhesive assessments are expected, it is concluded that fast release of the spermicide and sustained release of DOX from these pH-sensitive hydrogels make them promising candidates for localized delivery of therapeutic agents through intravaginal administration.

Acknowledgements The authors would like to thank Bailey Howe library at UVM and OCEM at Otago University for their resources.

Compliance with ethical standards

Conflict of interest The authors declare that they have no conflict of interest.

References

1. Hussain A, Ahsan F. The vagina as a route for systemic drug delivery. J Control Release. 2005;103:301–13.
2. Alexander NJ, Baker E, Kaptein M, Karck U, Miller L, Zampaglione E. Why consider vaginal drug administration? Fertil Steril. 2004;82:1–12.
3. Machado RM, Palmeira-De-Oliveira A, Martinez-De-Oliveira J, Palmeira-De-Oliveira R. Vaginal films for drug delivery. J Pharm Sci. 2013;102:2069–81.
4. Ensign LM, Tang BC, Wang Y-Y, Tse TA, Hoen T, Cone R, et al. Mucus-penetrating nanoparticles for vaginal drug delivery protect against herpes simplex virus. Sci. Transl. Med. 2012;4. https://doi.org/10.1126/scitranslmed.3003453.
5. Yohe ST, Herrera VLM, Colson YL, Grinstaff MW. 3D superhydrophobic electrospun meshes as reinforcement materials for sustained local drug delivery against colorectal cancer cells. J Control Release. 2012;162:92–101.
6. Wolinsky JB, Colson YL, Grinstaff MW. Local drug delivery strategies for cancer treatment: gels, nanoparticles, polymeric films, rods, and wafers. J Control Release. 2012;159:14–26.
7. Harwood B, Mishell DR Jr. Contraceptive vaginal rings. Semin Reprod Med. 2001;19:381–90.
8. Thurman AR, Clark MR, Hurlburt JA, Doncel GF. Intravaginal rings as delivery systems for microbicides and multipurpose prevention technologies. Int J Womens Health. 2013;5:695–708.
9. Loxley A, Mitchnick M, Okoh O, McConnell J, Goldman L, Morgan C, et al. Ethylene vinyl acetate intravaginal rings for the simultaneous delivery of the antiretroviral UC781 and contraceptive levonorgestrel. Drug Deliv Transl Res. 2011;1:247–55.
10. Malcolm RK, Forbes CJ, Geer L, Veazey RS, Goldman L, Klasse PJ, et al. Pharmacokinetics and efficacy of a vaginally administered maraviroc gel in rhesus macaques. J Antimicrob Chemother. 2013;68:678–83.
11. Johnson TJ, Srinivasan P, Albright TH, Watson-Buckheit K, Rabe L, Martin A, et al. Safe and sustained vaginal delivery of pyrimidinedione HIV-1 inhibitors from polyurethane intravaginal rings. J Antimicrob Chemother. 2012;56:1291–9.
12. Sitruk-Ware R, Nath A, Mishell DR. Contraception technology: past, present and future. Contraception. 2013;87:319–30.
13. Clifford GM, Smith JS, Plummer M, Muñoz N, Franceschi S. Human papillomavirus types in invasive cervical cancer worldwide: a meta-analysis. Br J Cancer. 2003;88:63.
14. Gupta S, Gupta MK. Possible role of nanocarriers in drug delivery against cervical cancer. Nano Rev Exp. 2017;8:1335567.
15. Ghaemmaghami F, Behtash N, Yarandi F, Moosavi A, Modares M, Toogeh G, et al. First-line chemotherapy with 5-FU and platinum for advanced and recurrent cancer of the cervix: a phase II study. J Obstet Gynaecol. 2003;23:422–5.
16. Robati M, Holtz D, Dunton CJ. A review of topotecan in combination chemotherapy for advanced cervical cancer. Ther Clin Risk Manag. 2008;4:213–8.
17. Zeng X, Tao W, Mei L, Huang L, Tan C, Feng S-S. Cholic acid-functionalized nanoparticles of star-shaped PLGA-vitamin E TPGS copolymer for docetaxel delivery to cervical cancer. Biomaterials. 2013;34:6058–67.
18. Miyamoto T, Takabe Y, Watanabe M, Terasima T. Effectiveness of a sequential combination of bleomycin and mitomycin-C on an advanced cervical cancer. Cancer. 1978;41:403–14.
19. Valet P, Senard JM, Devedjian JC, Planat V, Salomon R, Voisin T, et al. Characterization and distribution of alpha 2-adrenergic receptors in the human intestinal mucosa. J Clin Investig. 1993;91:2049–57.
20. Omura GA, Hubbard J, Hatch K. Chemotherapy of cervix cancer with doxorubicin and cisplatin. A phase I pilot study of the Gynecologic Oncology Group. Am J Clin Oncol. 1985;8:347–9.
21. Petrou I. Hormonal therapies offer females a targeted acne TX. Dermatol Times. 2007;28:2–S10, S3.
22. Welling LL. Psychobehavioral effects of hormonal contraceptive use. Evol Psychol. 2013;11:718–42.
23. Smith JS, Green J, Berrington de Gonzalez A, Appleby P, Peto J, Plummer M, et al. Cervical cancer and use of hormonal contraceptives: a systematic review. Lancet. 2003;361:1159–67.
24. Moreno V, Bosch FX, Muñoz N, Meijer CJLM, Shah KV, Walboomers JMM, et al. Effect of oral contraceptives on risk of cervical cancer in women with human papillomavirus infection: the IARC multicentric case-control study. Lancet. 2002;359:1085–92.
25. Han YA, Singh M, Saxena BB. Development of vaginal rings for sustained release of nonhormonal contraceptives and anti-HIV agents. Contraception. 2007;76:132–8.
26. Saxena BB, Singh M, Gospin RM, Chu CC, Ledger WJ. Efficacy of nonhormonal vaginal contraceptives from a hydrogel delivery system. Contraception. 2004;70:213–9.
27. Jalalvandi E, Hanton LR, Moratti SC. Schiff-base based hydrogels as degradable platforms for hydrophobic drug delivery. Eur Polym J. 2017;90:13–24.
28. Liu L, Yao W, Rao Y, Lu X, Gao J. pH-responsive carriers for oral drug delivery: challenges and opportunities of current platforms. Drug Deliv. 2017;24:569–81.
29. Grassi G, Farra R, Caliceti P, Guarnieri G, Salmaso S, Carenza M, et al. Temperature-sensitive hydrogels. Am J Drug Deliv. 2005;3:239–51.

30. Anseth KS, Metters AT, Bryant SJ, Martens PJ, Elisseeff JH, Bowman CN. In situ forming degradable networks and their application in tissue engineering and drug delivery. J Control Release. 2002;78:199–209.
31. Casettari L, Vllasaliu D, Castagnino E, Stolnik S, Howdle S, Illum L. PEGylated chitosan derivatives: synthesis, characterizations and pharmaceutical applications. Progress Polym Sci. 2012;37:659–85.
32. Deacon MP, Davis SS, White RJ, Nordman H, Carlstedt I, Errington N, et al. Are chitosan–mucin interactions specific to different regions of the stomach? Velocity ultracentrifugation offers a clue. Carbohydr Polym. 1999;38:235–8.
33. Acarturk F. Mucoadhesive vaginal drug delivery systems. Recent Pat Drug Deliv Formul. 2009;3:193–205.
34. Rençber S, Karavana SY, Şenyiğit ZA, Eraç B, Limoncu MH, Baloğlu E. Mucoadhesive in situ gel formulation for vaginal delivery of clotrimazole: formulation, preparation, and in vitro/in vivo evaluation. Pharm Dev Technol. 2017;22:551–61.
35. Clarke MA, Rodriguez AC, Gage JC, Herrero R, Hildesheim A, Wacholder S, et al. A large, population-based study of age-related associations between vaginal pH and human papillomavirus infection. BMC Infect Dis. 2012;12:33.
36. Krauss-Silva L, Almada-Horta A, Alves MB, Camacho KG, Moreira MEL, Braga A. Basic vaginal pH, bacterial vaginosis and aerobic vaginitis: prevalence in early pregnancy and risk of spontaneous preterm delivery, a prospective study in a low socioeconomic and multiethnic South American population. BMC Pregnancy Childbirth. 2014;14:107.
37. Kato Y, Onishi H, Machida Y. N-succinyl-chitosan as a drug carrier: water-insoluble and water-soluble conjugates. Biomaterials. 2004;25:907–15.
38. Aiping Z, Tian C, Lanhua Y, Hao W, Ping L. Synthesis and characterization of N-succinyl-chitosan and its self-assembly of nanospheres. Carbohydr Polym. 2006;66:274–9.
39. Jalalvandi E, Hanton LR, Moratti SC. Preparation of a pH sensitive hydrogel based on dextran and polyhydrazide for release of 5-flurouracil, an anticancer drug. J Drug Deliv Sci Technol. 2018;44:146–52.
40. Bae Y, Kataoka K. Intelligent polymeric micelles from functional poly(ethylene glycol)-poly(amino acid) block copolymers. Adv Drug Deliv Rev. 2009;61:768–84.
41. Xu W, He X, Zhong M, Hu X, Xiao Y. A novel pH-responsive hydrogel based on natural polysaccharides for controlled release of protein drugs. RSC Adv. 2015;5:3157–67.
42. Jalalvandi E, Cabral J, Hanton LR, Moratti SC. Cyclodextrin-polyhydrazine degradable gels for hydrophobic drug delivery. Mater Sci Eng C. 2016;69:144–53.
43. Kamoun EA. N-succinyl chitosan–dialdehyde starch hybrid hydrogels for biomedical applications. J Adv Res. 2016;7:69–77.
44. Horkay F, Han M-H, Han IS, Bang I-S, Magda JJ. Separation of the effects of pH and polymer concentration on the swelling pressure and elastic modulus of a pH-responsive hydrogel. Polymer. 2006;47:7335–8.
45. Yang B, Li X, Shi S, Kong X, Guo G, Huang M, et al. Preparation and characterization of a novel chitosan scaffold. Carbohydr Polym. 2010;80:860–5.
46. Yan C, Chen D, Gu J, Hu H, Zhao X, Qiao M. Preparation of N-succinyl-chitosan and their physical-chemical properties as a novel excipient. Yakugaku Zasshi. 2006;126:789–93.
47. Bashir S, Teo YY, Naeem S, Ramesh S, Ramesh K. pH responsive N-succinyl chitosan/poly(acrylamide-co-acrylic acid) hydrogels and in vitro release of 5-fluorouracil. PLoS ONE. 2017;12:e0179250.
48. Gipson IK. Mucins of the human endocervix. Front Biosci. 2001;6:D1245–55.
49. Xiao N, Liang H, Lu J. Degradable and biocompatible aldehyde-functionalized glycopolymer conjugated with doxorubicinvia acid-labile Schiff base linkage for pH-triggered drug release. Soft Matter. 2011;7:10834–40.
50. Ball C, Krogstad E, Chaowanachan T, Woodrow KA. Drug-eluting fibers for HIV-1 inhibition and contraception. PLoS ONE. 7:e49792.
51. Hong CY, Lee MF, Lai LJ, Wang CP. Effect of lipid peroxidation on beating frequency of human sperm tail. Andrologia. 1994;26:61–5.
52. Jones R, Mann T. Lipid peroxides in spermatozoa; formation, role of plasmalogen, and physiological significance. Proc R Soc Lond Ser B Biol Sci. 1976;193:317–33.
53. Calamera JC, Giovenco P, Quiros MC, Brugo S, Dondero F, Nicholson RF. Effect of lipid peroxidation upon human spermatic adenosinetriphosphate (ATP). Relationship with motility, velocity and linearity of the spermatozoa. Andrologia. 1989;21:48–54.